R-2392

H.-J. Kretzschmar[1]
Department of Technical Thermodynamics, University of Applied Sciences of Zittau and Gorlitz, P. O. Box 1455, D-02754 Zittau, Germany
e-mail: hj.kretzschmar@hs-zigr.de

J. R. Cooper
Department of Engineering, Queen Mary University of London, London, UK

A. Dittmann
Department of Technical Thermodynamics, Technical University of Dresden, Dresden, Germany

D. G. Friend
Physical and Chemical Properties Division, National Institute of Standards and Technology, Boulder, CO

J. S. Gallagher
Physical and Chemical Properties Division, National Institute of Standards and Technology, Gaithersburg, MD

K. Knobloch
Department of Technical Thermodynamics, University of Applied Sciences of Zittau and Gorlitz, P.O. Box 1455, D-02754 Zittau, Germany

R. Mareš
Department of Thermodynamics, University of West Bohemia, Plzeň, Czech Republic

K. Miyagawa
Tokyo, Japan

I. Stöcker
Department of Technical Thermodynamics, University of Applied Sciences of Zittau and Gorlitz, P.O. Box 1455, D-02754 Zittau, Germany

J. Trübenbach
Department of Technical Thermodynamics, Technical University of Dresden, Dresden, Germany

W. Wagner
Lehrstuhl für Thermodynamik, Ruhr-Universität Bochum, Bochum, Germany

Th. Willkommen
Department of Technical Thermodynamics, Technical University of Dresden, Dresden, Germany

Supplementary Backward Equations for Pressure as a Function of Enthalpy and Entropy $p(h,s)$ to the Industrial Formulation IAPWS-IF97 for Water and Steam

In modeling steam power cycles, thermodynamic properties as functions of the variables enthalpy and entropy are required in the liquid and the vapor regions. It is difficult to perform these calculations with IAPWS-IF97, because they require two-dimensional iterations calculated from the IAPWS-IF97 fundamental equations. While these calculations are not frequently required, the relatively large computing time required for two-dimensional iteration can be significant in process modeling. Therefore, the International Association for the Properties of Water and Steam (IAPWS) adopted backward equations for pressure as a function of enthalpy and entropy $p(h,s)$ as a supplement to the IAPWS Industrial Formulation 1997 for the Thermodynamic Properties of Water and Steam (IAPWS-IF97) in 2001. These $p(h,s)$ equations are valid in the liquid region 1 and the vapor region 2. With pressure p, temperature $T(h,s)$ can be calculated from the IAPWS-IF97 backward equations $T(p,h)$. By using the $p(h,s)$ equations, the two dimensional iterations of the IAPWS-IF97 basic equations can be avoided. The numerical consistency of pressure and temperature obtained in this way is sufficient for most heat cycle calculations. This paper summarizes the need and the requirements for the $p(h,s)$ equations and gives complete numerical information about the equations. Moreover, the achieved quality of the equations and their use in the calculation of the backward function $T(h,s)$ is presented. The three aspects, numerical consistency with the IAPWS-IF97 basic equations, consistency along subregion boundaries, and computational speed important for industrial use are discussed. [DOI: 10.1115/1.1915392]

1 Introduction

In 1997 the International Association for the Properties of Water and Steam (IAPWS) adopted the IAPWS Industrial Formulation 1997 for the Thermodynamic Properties of Water and Steam (IAPWS-IF97) [1,2]. This set of equations contains fundamental equations, saturation equations, and equations for the most often used backward functions $T(p,h)$ and $T(p,s)$ valid in liquid region 1 and vapor region 2; see Fig. 1.

In modeling power cycles and steam turbines, the backward functions $p(h,s)$ and $T(h,s)$ are also required, though not as often as $T(p,h)$ and $T(p,s)$. Table 1 contains the relative frequency of

[1]To whom correspondence should be addressed.

Submitted to ASME for publication in the JOURNAL OF ENGINEERING FOR GAS TURBINES AND POWER. Manuscript received October 20, 2003; final manuscript received June 22, 2004. Editor: L. S. Langston.

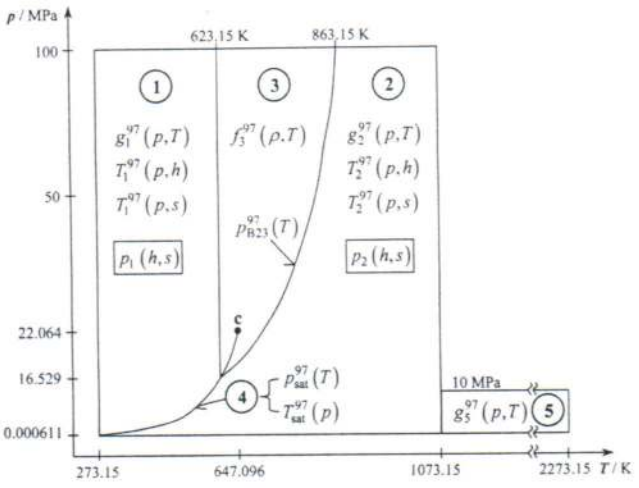

Fig. 1 Range of validity and equations of IAPWS-IF97, and presented backward equations $p(h,s)$

use of the backward functions $p(h,s)$ and $T(h,s)$ in comparison with $T(p,h)$ and $T(p,s)$ determined as a result of an international survey [3].

Although the functions $p(h,s)$ and $T(h,s)$ are seldom used in modeling power cycles, the computing time to calculate them from the IAPWS-IF97 basic equations is very high [4]. The reason is that two-dimensional iterations from $h^{97}(p,T)$ and $s^{97}(p,T)$ are necessary to calculate $p(h,s)$ and $T(h,s)$, where $h^{97}(p,T)$ and $s^{97}(p,T)$ are derivatives of the IAPWS-IF97 fundamental equations $g^{97}(p,T)$.

Therefore, IAPWS decided to develop backward equations $p(h,s)$ for the IAPWS-IF97 regions 1 and 2 (see Fig. 1). With pressure p, temperature T can be calculated from the IAPWS-IF97 backward equations $T^{97}(p,h)$ or $T^{97}(p,s)$.

The $p(h,s)$ equations were adopted by IAPWS at its meeting in Gaithersburg (USA), September 2001, under the name "Supplementary Release on Backward Equations for Pressure as a Function of Enthalpy and Entropy $p(h,s)$ to the IAPWS Industrial Formulation 1997 for the Thermodynamic Properties of Water and Steam [5]." This article provides the technical documentation for the equations.

2 Numerical Consistency Requirements

The backward equations $p(h,s)$ that should be developed have to be numerically consistent with the IAPWS-IF97 equations $h^{97}(p,T)$ and $s^{97}(p,T)$ derived from the Gibbs equation $g^{97}(p,T)$, as shown in Fig. 2.

The permissible value of Δp_{tol} can be determined based on the numerical consistency of the IAPWS-IF97 backward equations $T^{97}(p,h)$ and $T^{97}(p,s)$ using the total differential:

$$\Delta p_{tol} = \left(\frac{\partial p}{\partial h}\right)_s \Delta h_{tol} + \left(\frac{\partial p}{\partial s}\right)_h \Delta s_{tol}, \qquad (1)$$

where $(\partial p/\partial h)_s$ and $(\partial p/\partial s)_h$ are derivatives calculated from the IAPWS-IF97 basic equations [6] and Δh_{tol} and Δs_{tol} values set up by IAPWS when developing the IAPWS-IF97 [7].

Table 1 Relative frequency of use of important backward functions in process modeling

	$p(h,s)$ and $T(h,s)$	$T(p,h)$	$T(p,s)$
Liquid region	0.5%	3.2%	1.1%
Vapor region	1.0%	12.4%	6.1%

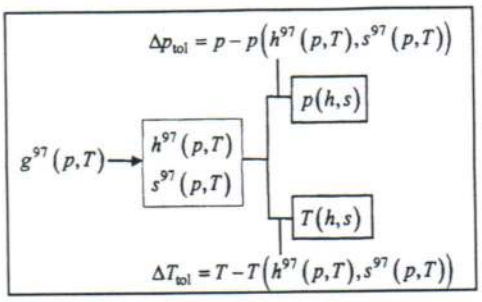

Fig. 2 Numerical consistency relations of the backward functions $p(h,s)$ and $T(h,s)$ with the IAPWS-IF97 equations $h^{97}(p,T)$ and $s^{97}(p,T)$

These Δh_{tol} and Δs_{tol} values are results of an international survey made among power plant companies and related industries. In order to be on the safe side, only the smaller of both summands of Eq. (1) was taken for determining Δp_{tol} in each region.

Table 2 shows the resulting numerical consistencies Δp_{tol} for the liquid region 1 and the vapor region 2. In region 2, the numerical consistency requirement is higher for entropies greater than $s = 5.85\ \text{kJ kg}^{-1}\ \text{K}^{-1}$. The values of Δp_{tol} had to be kept by the developed equations $p(h,s)$.

For the numerical consistency ΔT_{tol} of the backward function $T(h,s)$, Table 2 contains the same values IAPWS set up for the backward equations $T^{97}(p,h)$ and $T^{97}(p,s)$ when developing IAPWS-IF97 [8].

3 Development of the $p(h,s)$ Equations

A short computing time was one of the most important criteria for developing IAPWS-IF97 and also for the supplementary $p(h,s)$ backward equations. Investigations during the development of IAPWS-IF97 showed that polynomials in the form of a series of additions and multiplications are favorable as basic terms [9]. Therefore the following general functional expression was used:

$$\frac{p(h,s)}{p^*} = \sum_i n_i \left(\frac{h}{h^*} + b\right)^{I_i} \left(\frac{s}{s^*} + d\right)^{J_i}. \qquad (2)$$

Based on test calculations with Eq. (2), banks of terms with

$$I_i, J_i = 0 \cdots (1) \cdots 7, 8 \cdots (2) \cdots 22, 24 \cdots (4) \cdots 36$$

were generated. The structures of the final equations were found from Eq. (2) by using the approximation algorithm [10–13]. The algorithm combines a special modification of the structure-optimization method of Wagner [14] and Setzmann and Wagner [15] with elements for optimizing nonlinear parameters, automatic data weighting, and data-grid condensation. The modification takes into account the computing time needed to run the equation while it is being developed.

Table 2 Required numerical consistency values Δp_{tol} for $p(h,s)$ and ΔT_{tol} for $T(h,s)$

Region		$\lvert\Delta p\rvert_{tol}$	$\lvert\Delta T\rvert_{tol}$
1	$p \leq 2.5$ MPa	0.6%	25 mK
	$p > 2.5$ MPa	15 kPa	
2	$s < 5.85\ \text{kJ kg}^{-1}\ \text{K}^{-1}$	0.0088%	25 mK
	$s \geq 5.85\ \text{kJ kg}^{-1}\ \text{K}^{-1}$	0.0035%	10 mK

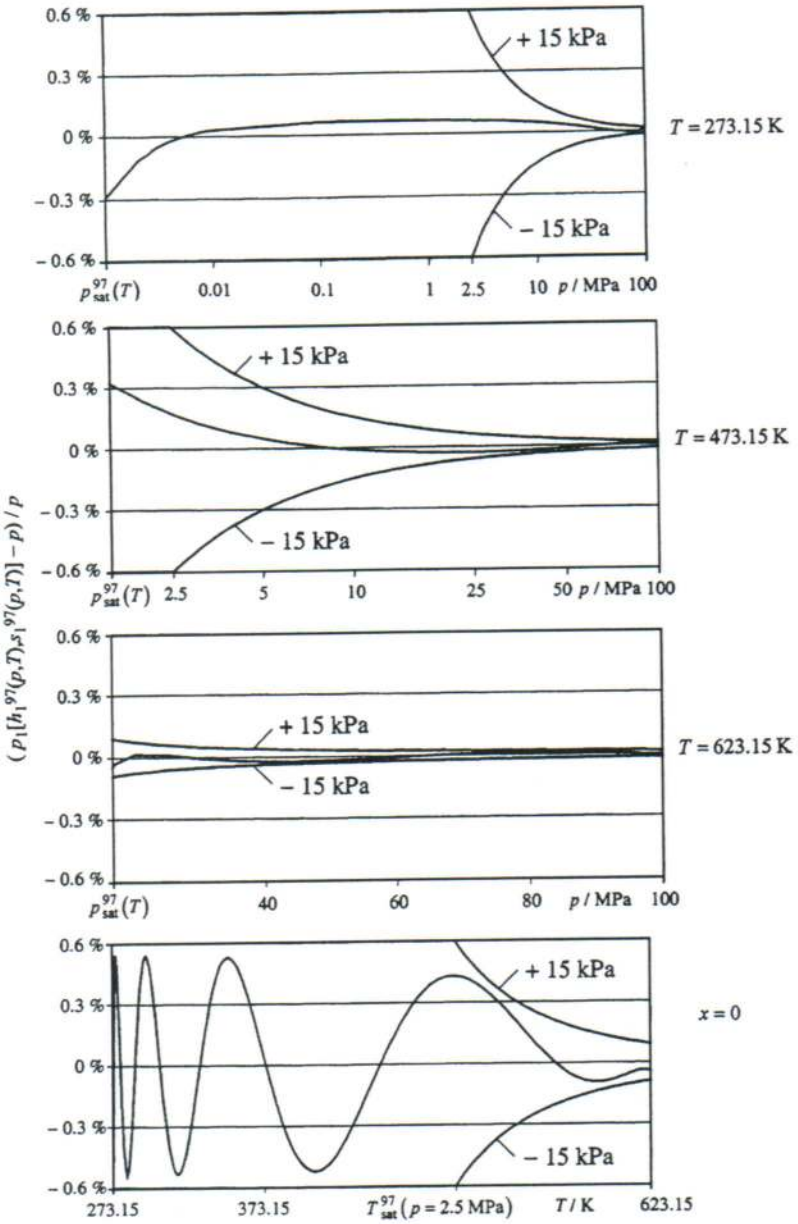

Fig. 3 Numerical consistency of equation $p(h,s)$, Eq. (3), with IAPWS-IF97 equation $g_1^{97}(p,T)$ for selected temperatures and along the saturated liquid line $x=0$

4 The Backward Equation $p(h,s)$ for Region 1

4.1 The Equation. The backward equation $p_1(h,s)$ for region 1 has the following dimensionless form:

$$\frac{p_1(h,s)}{p^*} = \pi(\eta,\sigma) = \sum_{i=1}^{19} n_i(\eta + 0.05)^{I_i}(\sigma + 0.05)^{J_i}, \qquad (3)$$

where $\pi = p/p^*$, $\eta = h/h^*$, and $\sigma = s/s^*$, with $p^* = 100$ MPa, $h^* = 3400$ kJ kg^{-1}, and $s^* = 7.6$ kJ kg^{-1} K^{-1}. The coefficients n_i and exponents I_i and J_i of Eq. (3) are listed in Table 6 of the Appendix.

4.1.1 Test values. To assist the user in computer-program verification of Eq. (3), Table 7 contains test values for calculated pressures.

4.1.2 Development of Eq. (3). Equation (3) has been developed based on Eq. (2). The reducing parameters p^*, h^*, and s^* are the maximum values of the range of validity of the equation. The shifting parameters b and d were determined by optimization. The exponents I_i, J_i, and the coefficients n_i are results of the structure optimization. In the optimization process, Eq. (3) was fitted to p-h-s values, where h and s had been calculated from the IAPWS-IF97 equation $g_1^{97}(p,T)$, for given values of p and T distributed as selected grid points over region 1. Details of the fitting processes are given in [10].

Table 3 Maximum differences and root-mean-square differences between pressures calculated from Eq. (3) and from IAPWS-IF97 equation $g_1^{97}(p,T)$ in comparison with the permissible differences

	$\lvert\Delta p\rvert_{tol}$	$\lvert\Delta p\rvert_{max}$	$(\Delta p)_{RMS}$
$p \le 2.5$ MPa	0.60%	0.55%	0.11%
$p > 2.5$ MPa	15 kPa	14 kPa	6 kPa

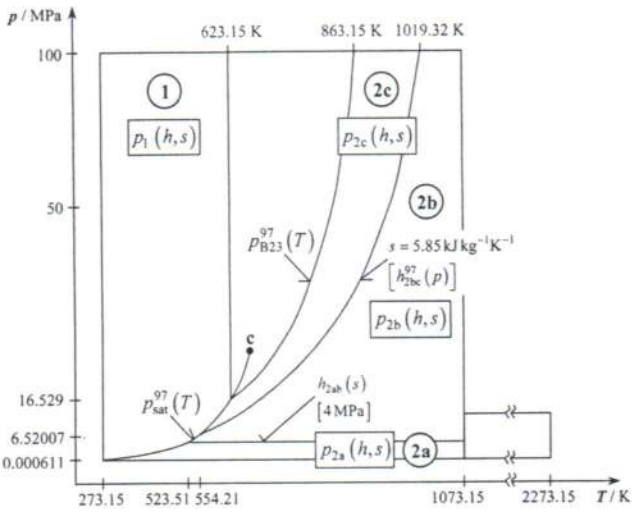

Fig. 4 Division of the IAPWS-IF97 region 2 into three subregions 2a, 2b, 2c for the backward equations $p(h,s)$

4.2 Numerical Consistency. The maximum pressure differences and related root-mean-square differences between $p_1(h,s)$, Eq. (3), and the IAPWS-IF97 fundamental equation $g_1^{97}(p,T)$ are listed in Table 3. For the calculation of the root-mean-square (RMS) values, 100 million points were generated for both pressure regions.

Thus, Eq. (3) meets the numerical consistency requirements of 0.6% for pressures less than or equal to 2.5 MPa and 15 kPa for pressures greater than 2.5 MPa. Figure 3 shows diagrams including relative pressure differences for selected temperatures and along the saturated liquid line $x=0$.

5 The Backward Equations $p(h,s)$ for Region 2

5.1 Subregions. Investigations in the process of developing the backward equations $p(h,s)$ for IAPWS-IF97 region 2 have shown that it was not possible to meet the numerical consistency values Δp_{tol} of Table 2 with a simple $p(h,s)$ equation. The problem was solved by dividing region 2 into three subregions 2a, 2b, and 2c (see Fig. 4). The division corresponds to that used for the IAPWS-IF97 backward equations $T(p,h)$ and $T(p,s)$.

The boundary between the subregions 2b and 2c is the entropy line $s=5.85$ kJ kg^{-1} K^{-1}. It can be tested directly because the specific entropy is a given parameter in the calculation of $p(h,s)$. If the given specific entropy s is greater than or equal to 5.85 kJ kg^{-1} K^{-1}, then the point of state to be calculated is situated in subregion 2b; otherwise it is in subregion 2c, see Fig. 4.

The boundary between subregions 2a and 2b corresponds to the isobar $p=4$ MPa. In order to decide which $p(h,s)$ equation, 2a or 2b, must be used for given values of h and s, the boundary equation $h_{2ab}(s)$, Eq. (4), has to be calculated. It is a polynomial of the third degree and reads

$$\frac{h_{2ab}(s)}{h^*} = \eta(\sigma) = n_1 + n_2\sigma + n_3\sigma^2 + n_4\sigma^3, \qquad (4)$$

where $\eta=h/h^*$ and $\sigma=s/s^*$, with $h^*=1$ kJ kg^{-1} and $s^*=1$ kJ kg^{-1} K^{-1}. The coefficients n_1 to n_4 of Eq. (4) are listed in Table 8.

The range of equation $h_{2ab}(s)$ is from $s''(p=4$ MPa) on the saturated vapor line to $s_2^{97}(p=4$ MPa, $T=1073.15$ K); see Fig. 4. Based on its simple form, Eq. (4) does not exactly describe the isobaric line $p=4$ MPa. The maximum deviation in pressure was determined as

$$|\Delta p_{2ab}|_{max} = |p_2^{97}[h_{2ab}(s_2^{97}), s_2^{97}] - 4\ \text{MPa}| = 22\ \text{kPa},$$

where p_2^{97} was obtained by iteration, and $s_2^{97}(p=4$ MPa, $T)$.

If the given specific enthalpy h is greater than $h_{2ab}(s)$ calculated from the given specific entropy s, then the point of state to be calculated is situated in subregion 2b, otherwise it is in subregion 2a (see Fig. 4).

5.1.1 Test Values. For computer-program verification, Eq. (4) gives the following s-h point: $s=7$ kJ kg^{-1} K^{-1}, $h_{2ab}=3376.437\,884$ kJ kg^{-1}.

5.2 The Equations

5.2.1 Subregion 2a. The backward equation $p_{2a}(h,s)$ for subregion 2a in its dimensionless form reads as follows:

$$\frac{p_{2a}(h,s)}{p^*} = \pi(\eta,\sigma) = \left[\sum_{i=1}^{29} n_i(\eta-0.5)^{I_i}(\sigma-1.2)^{J_i}\right]^4, \qquad (5)$$

where $\pi=p/p^*$, $\eta=h/h^*$, and $\sigma=s/s^*$, with $p^*=4$ MPa, $h^*=4200$ kJ kg^{-1}, and $s^*=12$ kJ kg^{-1} K^{-1}. The coefficients n_i and exponents I_i and J_i of Eq. (5) are listed in Table 9.

5.2.2 Subregion 2b. The backward equation $p_{2b}(h,s)$ for subregion 2b in its dimensionless form reads as follows:

$$\frac{p_{2b}(h,s)}{p^*} = \pi(\eta,\sigma) = \left[\sum_{i=1}^{33} n_i(\eta-0.6)^{I_i}(\sigma-1.01)^{J_i}\right]^4, \qquad (6)$$

where $\pi=p/p^*$, $\eta=h/h^*$, and $\sigma=s/s^*$, with $p^*=100$ MPa, $h^*=4100$ kJ kg^{-1}, and $s^*=7.9$ kJ kg^{-1} K^{-1}. The coefficients n_i and exponents I_i and J_i of Eq. (6) are listed in Table 10.

5.2.3 Subregion 2c. The backward equation $p_{2c}(h,s)$ for subregion 2c in its dimensionless form reads as follows:

$$\frac{p_{2c}(h,s)}{p^*} = \pi(\eta,\sigma) = \left[\sum_{i=1}^{31} n_i(\eta-0.7)^{I_i}(\sigma-1.1)^{J_i}\right]^4, \qquad (7)$$

where $\pi=p/p^*$, $\eta=h/h^*$, and $\sigma=s/s^*$, with $p^*=100$ MPa, $h^*=3500$ kJ kg^{-1}, and $s^*=5.9$ kJ kg^{-1} K^{-1}. The coefficients n_i and exponents I_i and J_i of Eq. (7) are listed in Table 11.

Equations (5)–(7) are valid in the respective subregion 2a, 2b, and 2c. The boundaries between these subregions are defined in Sec. 5.1.

Table 4 Maximum differences and root-mean-square differences between pressures calculated from Eqs. (5)–(7) and from the IAPWS-IF97 equation $g_2^{97}(p,T)$ in comparison with the permissible differences

Subregion	Equation	$\lvert\Delta p/p\rvert_{tol}$	$\lvert\Delta p/p\rvert_{max}$	$(\Delta p/p)_{RMS}$
2a	(5)	0.0035%	0.0029%	0.0013%
2b	(6)	0.0035%	0.0034%	0.0005%
2c	(7)	0.0088%	0.0063%	0.0010%

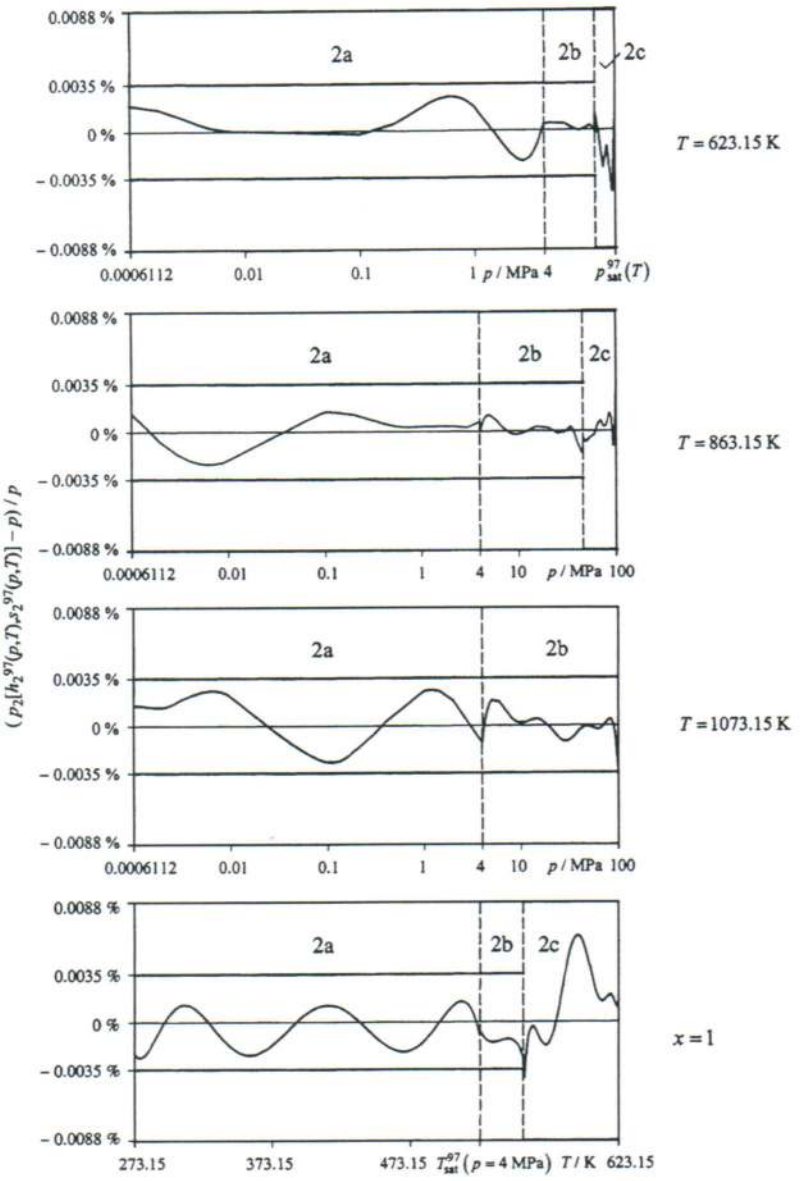

Fig. 5 Numerical consistency of equations $p(h,s)$, Eqs. (5)–(7), with the IAPWS-IF97 equation $g_2^{97}(p,T)$ for selected temperatures and along the saturated vapor line $x=1$

5.2.4 Test Values. To assist the user in computer-program verification of Eqs. (5)–(7), Table 12 contains the test values for calculated pressures.

5.2.5 Development of Eqs. (5)–(7). Equations (5)–(7) have been developed based on Eq. (2). The reducing parameters p^*, h^*, and s^* are the maximum values of the range of validity of the equations. The shifting parameters b and d were determined by optimization. The exponents I_i, J_i, and the coefficients n_i are results of the structure optimization. In the optimization process Eqs. (5)–(7) were fitted to p-h-s values, where h and s had been calculated from the IAPWS-IF97 equation $g_2^{97}(p,T)$, for given values of p and T distributed as selected grid points over subregions 2a, 2b, and 2c. Details of the fitting processes are given in [10].

5.3 Numerical Consistency. The maximum percentage deviations for pressure and related root-mean-square values of the Eqs. (5)–(7) from the IAPWS-IF97 fundamental equation $g_2^{97}(p,T)$ in comparison with the permissible differences are listed in Table 4. The RMS values were calculated from 100 million points for each subregion.

The maximum percentage deviations are less than the permissible differences of 0.0035% for subregions 2a and 2b and 0.0088% for subregion 2c; see Table 2.

Figure 5 illustrates the numerical consistency for selected isotherms and the saturated vapor line $x=1$, where $p(h,s)$ is calculated from Eq. (5) for subregion 2a, from Eq. (6) for subregion 2b, and from Eq. (7) for subregion 2c.

Comparatively, the maximum pressure difference of older equations for $p(h,s)$ for superheated steam of Schwindt [16], and Dohrendorf and Schwindt [17] with the previous industrial standard, the IFC-67 [18], was 1%.

5.4 Consistency at Subregion Boundaries. The relative pressure differences between the two backward equations of the adjacent subregions are smaller than the required numerical con-

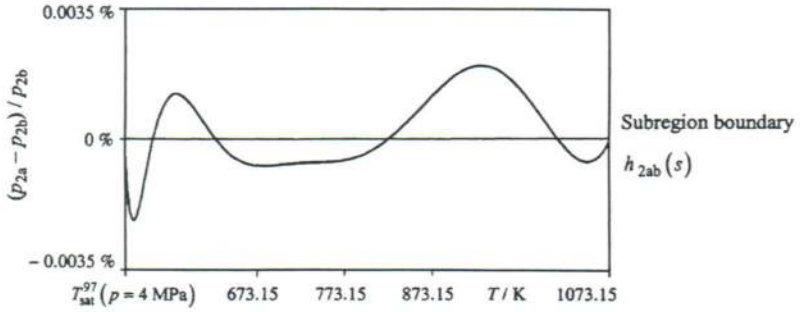

Fig. 6 Numerical consistency between $p_{2a}(h,s)$ and $p_{2b}(h,s)$ equations at the subregion boundary $h_{2ab}(s)$

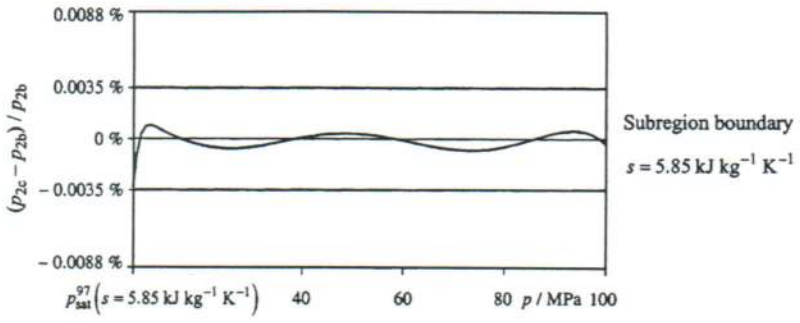

Fig. 7 Numerical consistency between $p_{2b}(h,s)$ and $p_{2c}(h,s)$ equations at the subregion boundary s=5.85 kJ kg^{-1} K^{-1}

sistencies with the IAPWS-IF97 equation.

At the boundary equation $h_{2ab}(s)$, Eq. (4), between subregions 2a and 2b (see Fig. 4), the maximum difference between the corresponding equations was determined as:

$$|\Delta p/p|_{max} = |p_{2a}(h,s) - p_{2b}(h,s)|/p_{2b}(h,s) = 0.0022\ \%\ .$$

Figure 6 illustrates the numerical consistency.

At the boundary line s=5.85 kJ kg^{-1} K^{-1} between subregions 2c and 2b, the maximum difference is

$$|\Delta p/p|_{max} = |p_{2c}(h,s) - p_{2b}(h,s)|/p_{2b}(h,s) = 0.0033\ \%\ .$$

Figure 7 illustrates the numerical consistency.

6 The Backward Function $T(h,s)$

6.1 Calculation of the Backward Function $T(h,s)$. The $p(h,s)$ equations described in Secs. 4 and 5 together with the backward equations $T^{97}(p,h)$ [the alternative use of the IAPWS-IF97 backward equations $T^{97}(p,s)$ leads to lower numerical consistency] of IAPWS-IF97 allow the determination of the temperature T from the enthalpy h and entropy s without iteration.

6.1.1 Liquid Region 1. For calculating T from a given h and s in region 1, the following steps should be made:

(1) Calculate pressure p using the equation $p_1(h,s)$, Eq. (3).
(2) Calculate temperature T using the IAPWS-IF97 equation $T_1^{97}(p,h)$ (see Fig. 1), where p was previously calculated.

6.1.2 Vapor Region 2. For calculating T from given h and s in region 2, the following steps should be made:

(1) Use the equation $h_{2ab}(s)$, Eq. (4), and the entropy line s =5.85 kJ kg^{-1} K^{-1} (see Fig. 4) to identify the subregion (2a, 2b, or 2c) for the given values of h and s. Then, calculate the pressure p for the subregion using the equations $p_{2a}(h,s)$, Eq. (5), or $p_{2b}(h,s)$, Eq. (6), or $p_{2c}(h,s)$, Eq. (7).
(2) Use the IAPWS-IF97 equation $h_{2bc}^{97}(p)$ and pressure line p =4 MPa to identify the IAPWS-IF97 subregion (2a, 2b, or 2c) for the given value of h and the calculated value of p. Then, calculate temperature T for the subregion using the IAPWS-IF97 backward equations $T_{2a}^{97}(p,h)$, $T_{2b}^{97}(p,h)$, or $T_{2c}^{97}(p,h)$.

6.2 Numerical Consistency. The maximum temperature differences and related root-mean-square differences between the calculated temperature and the IAPWS-IF97 fundamental equations $g_1^{97}(p,T)$ and $g_2^{97}(p,T)$ of regions 1 and 2 are listed in Table 5 together with the permissible differences. The temperature differences were calculated as:

$$\Delta T = (T_1^{97}(p_1(h_1^{97},s_1^{97}),h_1^{97}) - T) \text{ for region 1; and as}$$

$$\Delta T = (T_2^{97}(p_2(h_2^{97},s_2^{97}),h_2^{97}) - T) \text{ for subregions 2a, 2b, and 2c.}$$

The function T_2^{97} represents the calculation of $T(p,h)$ using the IAPWS-IF97 backward equations of region 2 including the determination in which subregion (2a, 2b, or 2c) the point is located. The RMS values were calculated from 100 million points for region 1 and subregions 2a, 2b, and 2c.

Figure 8 illustrates the numerical consistency for selected isotherms and along the saturated liquid line x=0 for region 1. Figure 9 shows the numerical consistency for selected isotherms and

Table 5 Maximum differences and root-mean-square differences between calculated temperatures and IAPWS-IF97 equations $g_1^{97}(p,T)$ and $g_2^{97}(p,T)$ in comparison with the permissible differences

Region/subregion	$\lvert\Delta T\rvert_{tol}$	$\lvert\Delta T\rvert_{max}$	$(\Delta T)_{RMS}$
1	25 mK	24.0 mK	13.4 mK
2a	10 mK	9.7 mK	3.0 mK
2b	10 mK	9.8 mK	4.0 mK
2c	25 mK	24.9 mK	10.3 mK

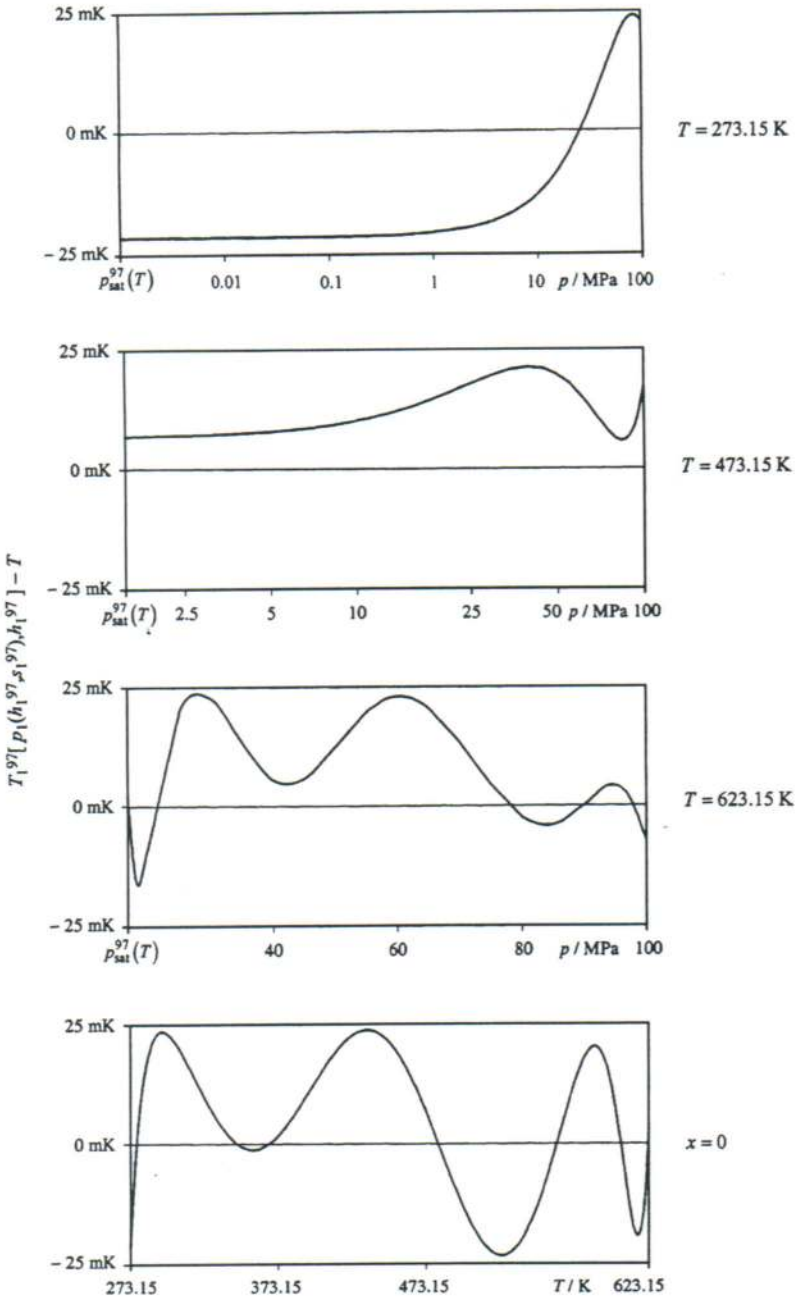

Fig. 8 Numerical consistency of the temperature calculated by $T_1^{97}[p_1(h^{97},s^{97}),h^{97}]$ with the IAPWS-IF97 equation $g_1^{97}(p,T)$ for selected temperatures and along the saturated liquid line $x=0$

along the saturated vapor line $x=1$ for region 2.

The deviations are less than the permissible differences of 10 mK for subregions 2a and 2b, and 25 mK for region 1 and subregion 2c; see Table 2. This means that the accuracy of the pressure calculated by the equations $p(h,s)$ is sufficient for calculating temperature from the IAPWS-IF97 backward equations $T^{97}(p,h)$.

Comparatively, the maximum temperature difference of the older equations $T(h,s)$ for superheated steam of Schwindt [16], and Dohrendorf and Schwindt [17] from the former industrial standard, the IFC-67 [18], was 2 K.

6.3 Consistency at Subregion Boundaries. The temperature differences between the two backward equations of the adjacent subregions have the following values.

6.3.1 Boundary between Subregions 2a and 2b. Along the boundary equation $h_{2ab}(s)$, Eq. (4), the maximum temperature difference was determined to be:

$$|\Delta T|_{max} = |T_2^{97}[p_{2a}(h_{2ab},s),h_{2ab}] - T_2^{97}[p_{2b}(h_{2ab},s),h_{2ab}]| = 6.7 \text{ mK},$$

where the function T_2^{97} represents the calculation of $T(p,h)$ from the IAPWS-IF97 backward equations of region 2 including the determination of the subregion (2a, 2b, or 2c). Figure 10 illustrates the numerical consistency. The peaks result from the fact that the boundary equation $h_{2ab}(s)$, Eq. (4), does not exactly de-

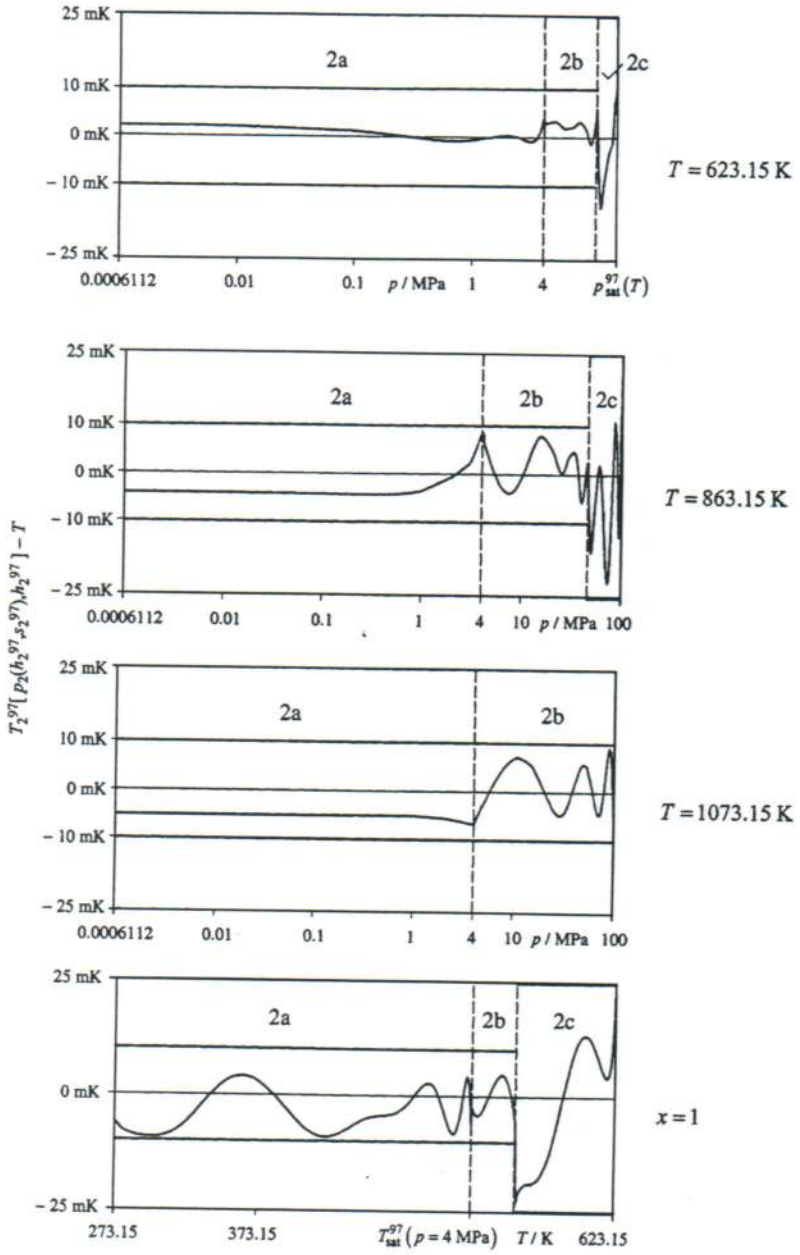

Fig. 9 Numerical consistency of the temperature calculated by $T_2^{97}[p_2(h^{97}, s^{97}), h^{97}]$ with IAPWS-IF97 equation $g_2^{97}(p, T)$ for selected temperatures and along the saturated vapor line $x=1$

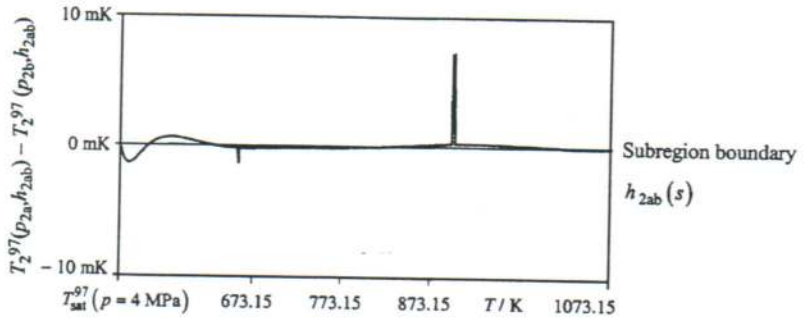

Fig. 10 Numerical consistency of $T_2(h, s)$ at the subregion boundary $h_{2ab}(s)$, Eq. (4)

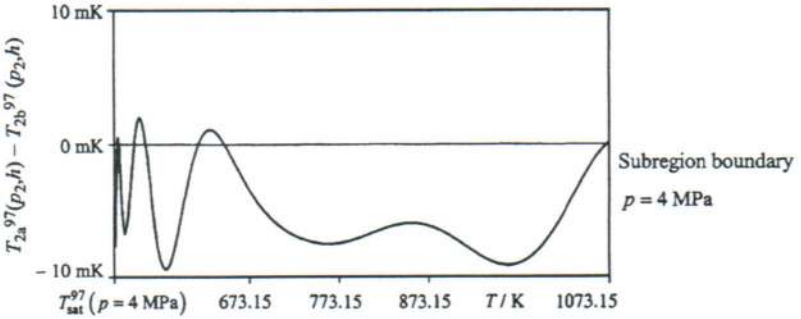

Fig. 11 Numerical consistency of $T_2(h,s)$ at the IAPWS-IF97 subregion boundary line p=4 MPa

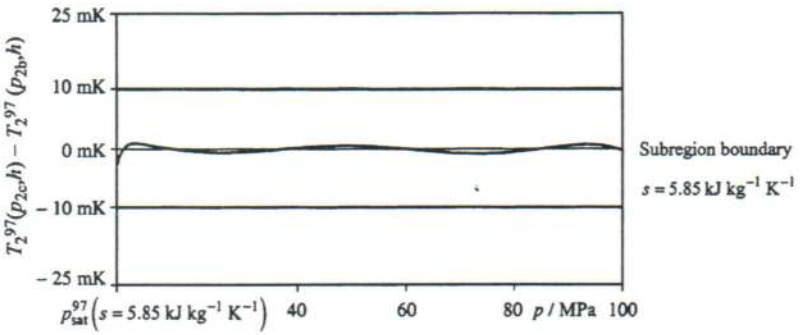

Fig. 12 Numerical consistency of $T_2(h,s)$ at the IAPWS-IF97 subregion boundary s=5.85 kJ kg^{-1} K^{-1}

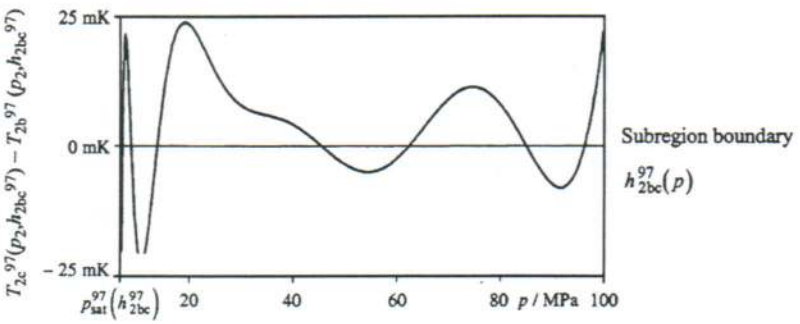

Fig. 13 Numerical consistency of $T_2(h,s)$ at the IAPWS-IF97 subregion boundary $h_{2bc}^{97}(p)$

scribe the isobaric line p=4 MPa.

Along the IAPWS-IF97 boundary line p=4 MPa, the following maximum difference was determined:

$$|\Delta T|_{max} = |T_{2a}^{97}(p_2(h_2^{97},s_2^{97}),h_2^{97}) - T_{2b}^{97}(p_2(h_2^{97},s_2^{97}),h_2^{97})| = 8.7\ \text{mK},$$

where $h_2^{97}(p=4\ \text{MPa},T)$ and $s_2^{97}(p=4\ \text{MPa},T)$. The function p_2 represents the calculation of $p(h,s)$ from the backward equations of region 2, Eqs. (5)–(7), and includes the determination of the subregion (2a, 2b, or 2c). Figure 11 illustrates the numerical consistency.

6.3.2 Boundary between Subregions 2b and 2c. Along the boundary line s=5.85 kJ kg^{-1} K^{-1}, the maximum temperature difference was determined to be:

$$|\Delta T|_{max} = |T_2^{97}[p_{2c}(h,s),h] - T_2^{97}[p_{2b}(h,s),h]| = 2.7\ \text{mK}.$$

Figure 12 illustrates the numerical consistency.

Along the IAPWS-IF97 boundary equation $h_{2bc}^{97}(p)$, the maximum temperature difference was determined to be

$$|\Delta T|_{max} = |T_{2c}^{97}(p_2(h_{2bc}^{97},s_2^{97}),h_{2bc}^{97}) - T_{2b}^{97}(p_2(h_{2bc}^{97},s_2^{97}),h_{2bc}^{97})|$$
$$= 21.8\ \text{mK}.$$

Figure 13 illustrates the numerical consistency.

7 Computing Time in Relation to IAPWS-IF97

A very important motivation for the development of the backward equations $p(h,s)$ was reducing the computing time to obtain the values of p and T from given values of h and s. In IAPWS-IF97, time-consuming iterative processes, e.g., the two-dimensional Newton method, are required. Using the $p(h,s)$ equations combined with the IAPWS-IF97 backward equations $T^{97}(p,h)$, the calculation speed is between 20 and 30 times faster than two-dimensional iteration of IAPWS-IF97 basic equations.

8 Application of the $p(h,s)$ Equations

The numerical consistency of p and T obtained in the described way is sufficient for most heat-cycle calculations. For users not

satisfied with the numerical consistency of the backward equations, the equations are still recommended for generating good starting points for an iterative process. It will significantly reduce the time to meet the convergence criteria of the iteration.

The backward equations $p(h,s)$ can be used only in their ranges of validity described in Secs. 4 and 5. They should not be used for determining any thermodynamic derivatives. Thermodynamic derivatives can be determined from the IAPWS-IF97 fundamental equations $g_1^{97}(p,T)$ and $g_2^{97}(p,T)$ as described in [6].

In any case, depending on the application, a conscious decision should be made whether to use the backward equations $p(h,s)$ or to calculate the corresponding values by iteration from the basic equations of IAPWS-IF97.

9 Summary

This paper has presented backward equations $p(h,s)$ for water and steam within the IAPWS-IF97 regions 1 and 2. With the determined pressure $p(h,s)$, the temperature $T(h,s)$ can be calculated from the IAPWS-IF97 backward equations $T^{97}(p,h)$. The numerical consistencies of calculated p and T values with those obtained from the IAPWS-IF97 basic equations $g^{97}(p,T)$ are sufficient for most applications in heat-cycle and steam-turbine calculations. For applications where the demands on numerical consistency are extremely high, iterations using the IAPWS-IF97 equations may still be necessary. In these cases, the equations $p(h,s)$ can be used for calculating very accurate starting values.

The calculations of $p(h,s)$ and $T(h,s)$ using the new equations are between 20 and 30 times faster than iteration from IAPWS-IF97.

Users who are interested in these equations can receive the source code upon request; see web site http://thermodynamics.hs-zigr.de.

Acknowledgments

The authors are indebted to other members of the following IAPWS groups: Working Group "Industrial Requirements and Solutions," and Working Group "Thermophysical Properties of Water and Steam." We are grateful to all IAPWS colleagues who contributed to the project of the development of the supplementary equations for the IAPWS Industrial Formulation 1997 for the Thermodynamic Properties of Water and Steam. Special thanks are due to A.H. Harvey for his very effective help. Two of us (H.-J.K. and K.K.) are particularly grateful to the Deutscher Akademischer Austausch Dienst (German Academic Exchange Service) for its financial support and to the National Institute of Standards and Technology, Physical and Chemical Properties Division, for arranging the working period of six months in Boulder, CO, USA.

Nomenclature

f = specific Helmholtz free energy
g = specific Gibbs free energy
h = specific enthalpy
p = pressure
s = specific entropy
T = absolute temperature [1]
x = vapor fraction
Δ = difference in any quantity
η = reduced enthalpy, $\eta=h/h^*$
π = reduced pressure, $\pi=p/p^*$
σ = reduced entropy, $\sigma=s/s^*$
n = coefficient
I = exponent
i = serial number

Superscripts

97 = quantity or equation of IAPWS-IF97
$*$ = reducing quantity
$''$ = saturated vapor state

Subscripts

1 = region 1
2 = region 2
2a = subregion 2a
2b = subregion 2b
2c = subregion 2c
2ab = boundary between subregions 2a and 2b
2bc = boundary between subregions 2b and 2c
3 = region 3
4 = region 4
5 = region 5
B23 = boundary between regions 2 and 3
max = maximum value of a quantity
RMS = root-mean-square value of a quantity
sat = saturation state
tol = tolerance of a quantity

Root-mean-square value:

$$\Delta z_{\mathrm{RMS}} = \sqrt{\frac{1}{m}\sum_{i=1}^{m}(\Delta z_i)^2}$$

where Δz_i can be either the absolute or relative difference between the corresponding quantities z; m is the number of Δz_i values (100 million points well distributed over the range of validity).

Appendix

This appendix contains Tables 6–12, in which the coefficients, exponents, and test values for computer-program verification are listed.

[1]Note: T denotes absolute temperature on the International Temperature Scale of 1990 (ITS-90).

Table 6 Coefficients and exponents of Eq. (3)

i	I_i	J_i	n_i	i	I_i	J_i	n_i
1	0	0	−0.691 997 014 660 582	11	1	4	$-0.319\,947\,848\,334\,300\times10^{3}$
2	0	1	$-0.183\,612\,548\,787\,560\times10^{2}$	12	1	6	$-0.928\,354\,307\,043\,320\times10^{3}$
3	0	2	$-0.928\,332\,409\,297\,335\times10^{1}$	13	2	0	$0.303\,634\,537\,455\,249\times10^{2}$
4	0	4	$0.659\,639\,569\,909\,906\times10^{2}$	14	2	1	$-0.650\,540\,422\,444\,146\times10^{2}$
5	0	5	$-0.162\,060\,388\,912\,024\times10^{2}$	15	2	10	$-0.430\,991\,316\,516\,130\times10^{4}$
6	0	6	$0.450\,620\,017\,338\,667\times10^{3}$	16	3	4	$-0.747\,512\,324\,096\,068\times10^{3}$
7	0	8	$0.854\,680\,678\,224\,170\times10^{3}$	17	4	1	$0.730\,000\,345\,529\,245\times10^{3}$
8	0	14	$0.607\,523\,214\,001\,162\times10^{4}$	18	4	4	$0.114\,284\,032\,569\,021\times10^{4}$
9	1	0	$0.326\,487\,682\,621\,856\times10^{2}$	19	5	0	$-0.436\,407\,041\,874\,559\times10^{3}$
10	1	1	$-0.269\,408\,844\,582\,931\times10^{2}$				

Table 7 Selected pressure values calculated from Eq. (3) for selected enthalpies and entropies

h, kJ kg^{-1}	s, kJ kg^{-1} K^{-1}	$p_1(h,s)$, MPa
0.001	0	$9.800\,980\,612 \times 10^{-4}$
90	0	$9.192\,954\,727 \times 10^{1}$
1500	3.4	$5.868\,294\,423 \times 10^{1}$

Table 8 Coefficients of Eq. (4)

i	n_i	i	n_i
1	$-0.349\,898\,083\,432\,139 \times 10^{4}$	3	$-0.421\,073\,558\,227\,969 \times 10^{3}$
2	$0.257\,560\,716\,905\,876 \times 10^{4}$	4	$0.276\,349\,063\,799\,944 \times 10^{2}$

Table 9 Coefficients and exponents of Eq. (5)

i	I_i	J_i	n_i	i	I_i	J_i	n_i
1	0	1	$-0.182\,575\,361\,923\,032 \times 10^{-1}$	16	1	22	$0.431\,757\,846\,408\,006 \times 10^{4}$
2	0	3	$-0.125\,229\,548\,799\,536$	17	2	3	$0.112\,894\,040\,802\,650 \times 10^{1}$
3	0	6	$0.592\,290\,437\,320\,145$	18	2	16	$0.197\,409\,186\,206\,319 \times 10^{4}$
4	0	16	$0.604\,769\,706\,185\,122 \times 10^{1}$	19	2	20	$0.151\,612\,444\,706\,087 \times 10^{4}$
5	0	20	$0.238\,624\,965\,444\,474 \times 10^{3}$	20	3	0	$0.141\,324\,451\,421\,235 \times 10^{-1}$
6	0	22	$-0.298\,639\,090\,222\,922 \times 10^{3}$	21	3	2	$0.585\,501\,282\,219\,601$
7	1	0	$0.512\,250\,813\,040\,750 \times 10^{-1}$	22	3	3	$-0.297\,258\,075\,863\,012 \times 10^{1}$
8	1	1	$-0.437\,266\,515\,606\,486$	23	3	6	$0.594\,567\,314\,847\,319 \times 10^{1}$
9	1	2	$0.413\,336\,902\,999\,504$	24	3	16	$-0.623\,656\,565\,798\,905 \times 10^{4}$
10	1	3	$-0.516\,468\,254\,574\,773 \times 10^{1}$	25	4	16	$0.965\,986\,235\,133\,332 \times 10^{4}$
11	1	5	$-0.557\,014\,838\,445\,711 \times 10^{1}$	26	5	3	$0.681\,500\,934\,948\,134 \times 10^{1}$
12	1	6	$0.128\,555\,037\,824\,478 \times 10^{2}$	27	5	16	$-0.633\,207\,286\,824\,489 \times 10^{4}$
13	1	10	$0.114\,144\,108\,953\,290 \times 10^{2}$	28	6	3	$-0.558\,919\,224\,465\,760 \times 10^{1}$
14	1	16	$-0.119\,504\,225\,652\,714 \times 10^{3}$	29	7	1	$0.400\,645\,798\,472\,063 \times 10^{-1}$
15	1	20	$-0.284\,777\,985\,961\,560 \times 10^{4}$				

Table 10 Coefficients and exponents of Eq. (6)

i	I_i	J_i	n_i	i	I_i	J_i	n_i
1	0	0	$0.801\,496\,989\,929\,495 \times 10^{-1}$	18	3	12	$0.336\,972\,380\,095\,287 \times 10^{8}$
2	0	1	$-0.543\,862\,807\,146\,111$	19	4	1	$-0.586\,634\,196\,762\,720 \times 10^{3}$
3	0	2	$0.337\,455\,597\,421\,283$	20	4	16	$-0.221\,403\,224\,769\,889 \times 10^{11}$
4	0	4	$0.890\,555\,451\,157\,450 \times 10^{1}$	21	5	1	$0.171\,606\,668\,708\,389 \times 10^{4}$
5	0	8	$0.313\,840\,736\,431\,485 \times 10^{3}$	22	5	12	$-0.570\,817\,595\,806\,302 \times 10^{9}$
6	1	0	$0.797\,367\,065\,977\,789$	23	6	1	$-0.312\,109\,693\,178\,482 \times 10^{4}$
7	1	1	$-0.121\,616\,973\,556\,240 \times 10^{1}$	24	6	8	$-0.207\,841\,384\,633\,010 \times 10^{7}$
8	1	2	$0.872\,803\,386\,937\,477 \times 10^{1}$	25	6	18	$0.305\,605\,946\,157\,786 \times 10^{13}$
9	1	3	$-0.169\,769\,781\,757\,602 \times 10^{2}$	26	7	1	$0.322\,157\,004\,314\,333 \times 10^{4}$
10	1	5	$-0.186\,552\,827\,328\,416 \times 10^{3}$	27	7	16	$0.326\,810\,259\,797\,295 \times 10^{12}$
11	1	12	$0.951\,159\,274\,344\,237 \times 10^{5}$	28	8	1	$-0.144\,104\,158\,934\,487 \times 10^{4}$
12	2	1	$-0.189\,168\,510\,120\,494 \times 10^{2}$	29	8	3	$0.410\,694\,867\,802\,691 \times 10^{3}$
13	2	6	$-0.433\,407\,037\,194\,840 \times 10^{4}$	30	8	14	$0.109\,077\,066\,873\,024 \times 10^{12}$
14	2	18	$0.543\,212\,633\,012\,715 \times 10^{9}$	31	8	18	$-0.247\,964\,654\,258\,893 \times 10^{14}$
15	3	0	$0.144\,793\,408\,386\,013$	32	12	10	$0.188\,801\,906\,865\,134 \times 10^{10}$
16	3	1	$0.128\,024\,559\,637\,516 \times 10^{3}$	33	14	16	$-0.123\,651\,009\,018\,773 \times 10^{15}$
17	3	7	$-0.672\,309\,534\,071\,268 \times 10^{5}$				

Table 11 Coefficients and exponents of Eq. (7)

i	I_i	J_i	n_i	i	I_i	J_i	n_i
1	0	0	0.112 225 607 199 012	17	3	0	0.772 465 073 604 171
2	0	1	$-0.339\,005\,953\,606\,712\times10^{1}$	18	3	5	$0.463\,929\,973\,837\,746\times10^{5}$
3	0	2	$-0.320\,503\,911\,730\,094\times10^{2}$	19	3	8	$-0.137\,317\,885\,134\,128\times10^{8}$
4	0	3	$-0.197\,597\,305\,104\,900\times10^{3}$	20	3	16	$0.170\,470\,392\,630\,512\times10^{13}$
5	0	4	$-0.407\,693\,861\,553\,446\times10^{3}$	21	3	18	$-0.251\,104\,628\,187\,308\times10^{14}$
6	0	8	$0.132\,943\,775\,222\,331\times10^{5}$	22	4	18	$0.317\,748\,830\,835\,520\times10^{14}$
7	1	0	$0.170\,846\,839\,774\,007\times10^{1}$	23	5	1	$0.538\,685\,623\,675\,312\times10^{2}$
8	1	2	$0.373\,694\,198\,142\,245\times10^{2}$	24	5	4	$-0.553\,089\,094\,625\,169\times10^{5}$
9	1	5	$0.358\,144\,365\,815\,434\times10^{4}$	25	5	6	$-0.102\,861\,522\,421\,405\times10^{7}$
10	1	8	$0.423\,014\,446\,424\,664\times10^{6}$	26	5	14	$0.204\,249\,418\,756\,234\times10^{13}$
11	1	14	$-0.751\,071\,025\,760\,063\times10^{9}$	27	6	8	$0.273\,918\,446\,626\,977\times10^{9}$
12	2	2	$0.523\,446\,127\,607\,898\times10^{2}$	28	6	18	$-0.263\,963\,146\,312\,685\times10^{16}$
13	2	3	$-0.228\,351\,290\,812\,417\times10^{3}$	29	10	7	$-0.107\,890\,854\,108\,088\times10^{10}$
14	2	7	$-0.960\,652\,417\,056\,937\times10^{6}$	30	12	7	$-0.296\,492\,620\,980\,124\times10^{11}$
15	2	10	$-0.807\,059\,292\,526\,074\times10^{8}$	31	16	10	$-0.111\,754\,907\,323\,424\times10^{16}$
16	2	18	$0.162\,698\,017\,225\,669\times10^{13}$				

Table 12 Selected pressure values calculated from Eqs. (5)–(7) for selected enthalpies and entropies

Equation	h, kJ kg^{-1}	s, kJ kg^{-1} K^{-1}	p, MPa
$p_{2a}(h,s)$, Eq (5)	2800	6.5	1.371 012 767
	2800	9.5	$1.879\,743\,844\times10^{-3}$
	4100	9.5	$1.024\,788\,997\times10^{-1}$
$p_{2b}(h,s)$, Eq (6)	2800	6.0	4.793 911 442
	3600	6.0	$8.395\,519\,209\times10^{1}$
	3600	7.0	7.527 161 441
$p_{2c}(h,s)$, Eq (7)	2800	5.1	$9.439\,202\,060\times10^{1}$
	2800	5.8	8.414 574 124
	3400	5.8	$8.376\,903\,879\times10^{1}$

References

[1] International Association for the Properties of Water and Steam, 1997, "Release on the IAPWS Industrial Formulation 1997 for the Thermodynamic Properties of Water and Steam," IAPWS Release, IAPWS Secretariat, available at www.iapws.org.

[2] Wagner, W., Cooper, J. R., Dittmann, A., Kijima, J., Kretzschmar, H.-J., Kruse, A., Mareš, R., Oguchi, K., Sato, H., Stöcker, I., Šifner, O., Tanishita, I., Trübenbach, J., and Willkommen, Th., 2000, "The IAPWS Industrial Formulation 1997 for the Thermodynamic Properties of Water and Steam," J. Eng. Gas Turbines Power, **122**, pp. 150–182.

[3] Rukes, B., 1991, "Relative frequencies of use of property functions in process modeling," Report to the Subcommittee Industrial Calculations of IAPWS, Siemens KWU, Erlangen.

[4] Weber, I., 1997, "Test der neuen industriellen Formulierung für Routinen der Wasser-/Dampf-Zustandsgrößen (Test of the new industrial formulation for water and steam)," Report, Siemens Power Generation, Erlangen.

[5] International Association for the Properties of Water and Steam, 2001, "Supplementary Release on Backward Equations for Pressure as a Function of Enthalpy and Entropy $p(h,s)$ to the IAPWS Industrial Formulation 1997 for the Thermodynamic Properties of Water and Steam," IAPWS Release, IAPWS Secretariat, available at www.iapws.org.

[6] Kretzschmar, H.-J., Stöcker, I., Klinger, J., and Dittmann, A., 2000, "Calculation of Thermodynamic Derivatives for Water and Steam Using the New Industrial Formulation IAPWS-IF97," in Tremaine, P. R. et al., eds., "Steam, Water and Hydrothermal Systems: Physics and Chemistry Meeting the Needs of Industry," in Proceedings of the 13th International Conference on the Properties of Water and Steam, NRC Press, Ottawa, pp. 238–247.

[7] Rukes, B., and Wagner, W., 1991, "Final Set of Specifications for the New Industrial Formulation," in Dooley, B., ed., Minutes of the Meetings of the Executive Committee of the International Association for the Properties of Water and Steam, Tokyo 1991, IAPWS Secretariat, pp. 78–82.

[8] Rukes, B., 1994, "Specifications for Numerical Consistency," in Dooley, B., ed., Minutes of the Meetings of the Executive Committee of the International Association for the Properties of Water and Steam, Orlando 1994, IAPWS Secretariat, pp. 31–33.

[9] Kruse, A., and Wagner, W., 1998, "Neue Zustandsgleichungen für industrielle Anwendungen im technisch relevanten Zustandsgebiet von Wasser (New equations of state for water for industrial use)," *Fortschr.-Ber. VDI, Reihe 6*, Nr. 393, VDI-Verlag, Düsseldorf.

[10] Trübenbach, J., 1999, "Ein Algorithmus zur Aufstellung rechenzeitoptimierter Gleichungen für thermodynamische Zustandsgrößen (An algorithm for developing equations of state optimized regarding their computing time consumption)," *Fortschr.-Ber. VDI, Reihe 6*, Nr. 417, VDI-Verlag, Düsseldorf.

[11] Willkommen, Th., Kretzschmar, H.-J., and Dittmann, A., 1995, "An Algorithm for Setting up Numerically Consistent Forward and Backward Equations for Process Modeling," in White et al., eds., Physical Chemistry of Aqueous Systems, in Proceedings of the 12th International Conference on the Properties of Water and Steam, Begell House, New York, pp. 194–201.

[12] Willkommen, Th., 1995, "Ein Algorithmus zur Aufstellung numerisch konsistenter Gleichungen für die in Prozessmodellierungen benötigten thermodynamischen Umkehrfunktionen (An algorithm for developing numerically consistent backward equations for use in process modeling)," Dissertation Faculty of Mechanical Engineering, Technical University of Dresden, Dresden.

[13] Kretzschmar, H.-J., 1990, "Zur Aufbereitung und Darbietung thermophysikalischer Stoffdaten für die Energietechnik (The preparation and processing of thermophysical properties for power engineering)," Habilitation, Faculty of Mechanical Engineering, Technical University of Dresden, Dresden.

[14] Wagner, W., 1974, "Eine mathematisch statistische Methode zum Aufstellen thermodynamischer Gleichungen-gezeigt am Beispiel der Dampfdruckkurve reiner fluider Stoffe (A mathematical statistical method for developing equations of state-demonstration with the vapor pressure curves of pure fluids)," *Fortschr.-Ber. VDI, Reihe 3*, Nr. 39, VDI-Verlag, Düsseldorf.

[15] Setzmann, W., Wagner, W., 1989, "A New Method for Optimizing the Structure of Thermodynamic Correlation Equations," Int. J. Thermophys., **10**, pp. 1103–1126.

[16] Schwindt, H., 1978, "Neue Näherungsformeln für die Zustandsgrößen der Wasserdampfes in Abhängigkeit von Enthalpie und Entropie (New approximations for the properties of steam as a function of enthalpy and entropy)," Brennst.-Waerme-Kraft, **30**, pp. 30–32.

[17] Dohrendorf, E., and Schwindt, H., 1970, "Näherungsformeln für die Zustandsgrößen des Wasserdampfes in Abhängigkeit von Enthalpie und Entropie (Approximations for the properties of steam as a function of enthalpy and entropy)," Brennst.-Waerme-Kraft, **22**, pp. 578–583.

[18] International Formulation Committee of the 6th International Conference on the Properties of Steam, 1967, "The 1967 IFC Formulation for Industrial Use," Verein Deutscher Ingenieure, Düsseldorf.